# Lipophilic 2,5-Disubstituted Pyrroles from the Marine Sponge *Mycale* sp. Inhibit Mitochondrial Respiration and HIF-1 Activation

Shui-Chun Mao,[†] Yang Liu,[†] J. Brian Morgan,[†] Mika B. Jekabsons,[‡] Yu-Dong Zhou,*,[†] and Dale G. Nagle*,[†,§]

*Department of Pharmacognosy and Research Institute of Pharmaceutical Sciences, School of Pharmacy, University of Mississippi, University, Mississippi 38677, and Department of Biology, University of Mississippi, University, Mississippi 38677*
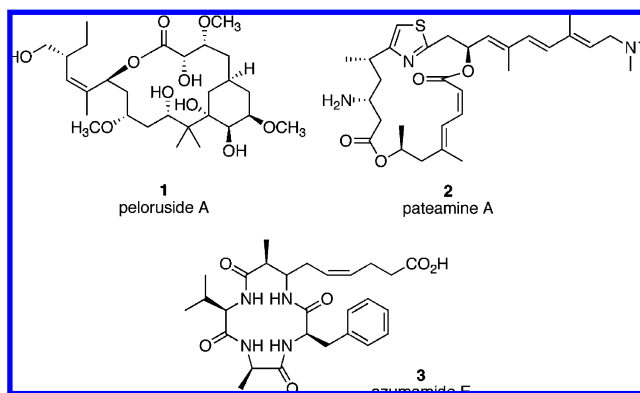
The lipid extract of the marine sponge *Mycale* sp. inhibited the activation of hypoxia-inducible factor-1 (HIF-1) in a human breast tumor T47D cell-based reporter assay. Bioassay-guided isolation and structure elucidation yielded 18 new lipophilic 2,5-disubstituted pyrroles and eight structurally related known compounds. The active compounds inhibited hypoxia-induced HIF activation with moderate potency ($IC_{50}$ values <10 $\mu$M). Mechanistic studies revealed that the active compounds suppressed mitochondrial respiration by blocking NADH-ubiquinone oxidoreductase (complex I) at concentrations that inhibited HIF-1 activation. Under hypoxic conditions, reactive oxygen species produced by mitochondrial complex III are believed to act as a signal of cellular hypoxia that leads to HIF-1$\alpha$ protein induction and activation. By inhibiting electron transport (or delivery) to complex III under hypoxic conditions, lipophilic *Mycale* pyrroles appear to disrupt mitochondrial ROS-regulated HIF-1 signaling.

Hypoxic regions arise in solid tumors when the existing blood vessels fail to meet the increased demand for oxygen from the rapidly proliferating malignant cells. Clinical studies indicate that the extent of tumor hypoxia correlates with advanced disease stages, malignant progression, treatment resistance, and poor prognosis.[1,2] Despite decades of drug discovery efforts, there is no approved drug that specifically targets tumor hypoxia. The focus of our antitumor hypoxia drug discovery research is to identify and characterize small molecule inhibitors of hypoxia-inducible factor-1 (HIF-1). The transcription factor HIF-1 is a heterodimer made up of two proteins: an oxygen-regulated HIF-1$\alpha$ subunit and a constitutively expressed HIF-1$\beta$/ARNT subunit. First discovered by Semenza and colleagues,[3,4] HIF-1 has become an important molecular target for anticancer drug discovery.[5–7] Under normoxic conditions, HIF-1 is inactivated due to the rapid degradation of the oxygen-regulated HIF-1$\alpha$ protein by the proteasome.[8,9] Both the prolyl hydroxylases that tag HIF-1$\alpha$ protein for degradation and the asparaginyl hydroxylase that inactivates HIF-1$\alpha$ protein utilize oxygen as a substrate and require ferrous iron ($Fe^{2+}$) as a cofactor.[10–14] Hypoxic exposure, treatment with hypoxia mimetics (i.e., iron chelators, transition metals, etc.), activation of oncogenes, and inactivation of tumor suppressor genes can lead to the stabilization and activation of HIF-1$\alpha$ protein and subsequent HIF-1 activation.[5–7] Upon activation, HIF-1 binds to the hypoxia-response element (HRE) located in the promoter regions of target genes and regulates gene expression. The activation of HIF-1-mediated signaling pathways results in enhanced cellular adaptation and survival under hypoxic conditions.[5–7] As in the case of tumor hypoxia, clinical observations have revealed that expression of the oxygen-regulated HIF-1$\alpha$ subunit also correlates with advanced disease stages, poor prognosis, and treatment resistance among cancer patients.[5–7] In animal-based preclinical studies, the inhibition of HIF-1 by various approaches (small molecule inhibitors, RNA antagonists, etc.) leads to the suppression of tumor growth.[15–17] Improved treatment outcomes have resulted when HIF-1 inhibition was combined with chemotherapeutic agents and/or radiation.[18–21] Agents that inhibit HIF-1 have entered early phase clinical trials for cancer: EZN-2968, a HIF-1$\alpha$ RNA antagonist; topotecan, a

natural product-derived topoisomerase-1/HIF-1 inhibitor; and PX-478, a small molecule that decreases HIF-1$\alpha$ gene expression.[22] Numerous drug discovery efforts are underway to identify and develop HIF-1 inhibitors for the treatment of cancer.[5–7]

Over 20 000 extracts of plants and marine organisms have been evaluated for natural products that inhibit HIF-1 activation in a T47D human breast tumor cell-based reporter assay.[23–25] The lipophilic extract of a Palau collection of the marine sponge *Mycale* sp. (Mycalidae) from the NCI Open Repository of marine invertebrate extracts inhibited hypoxia-induced HIF-1 activation in a 96-well plate-based reporter assay. A number of cytotoxic agents have been isolated from various *Mycale* spp. Representative *Mycale* metabolites with known antitumor mechanisms include the microtubule stabilizer peloruside A (**1**),[26–28] the translation inhibitor pateamine A (**2**), which disrupts the function of translation initiation factor eIF4A,[29–31] and the histone deacetylase (HDAC) inhibitor azumamide E (**3**).[32,33]



peloruside A (**1**)
pateamine A (**2**)
azumamide E (**3**)

Bioassay-guided isolation of the active *Mycale* sp. lipid extract afforded 18 new 5-alkylpyrrole-2-carbaldehyde metabolites, **4–21**, and eight structurally related known compounds, **22–29**.[34–36] Herein, this report describes the identification and characterization of 5-alkylpyrrole-2-carbaldehyde *Mycale* metabolites that inhibit HIF-1 activation. Further mechanistic investigation revealed that these compounds suppress tumor cell respiration at mitochondrial electron transport chain (ETC) complex I.

## Results and Discussion

In a human breast tumor T47D cell-based reporter assay,[23–25] a lipid extract of the sponge *Mycale* sp. inhibited hypoxia (1% $O_2$)-

* Corresponding authors. (Y.-D.Z.) Tel: (662) 915-7026. Fax: (662) 915-6975. E-mail: ydzhou@olemiss.edu. (D.G.N.) Tel: (662) 915-7026. Fax: (662) 915-6975. E-mail: dnagle@olemiss.edu.
† Department of Pharmacognosy.
‡ Department of Biology.
§ Research Institute of Pharmaceutical Sciences.
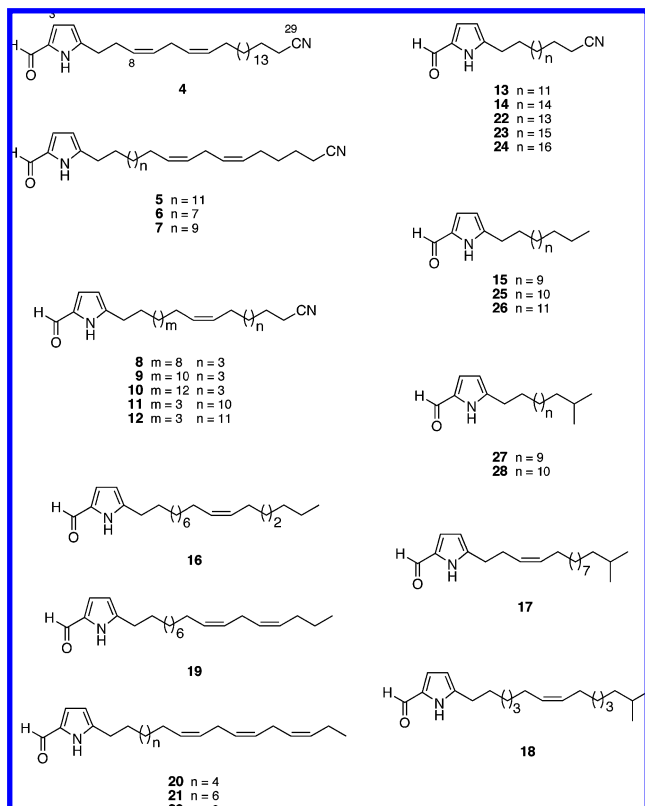
induced HIF-1 activation by 53% at 5 $\mu$g mL$^{-1}$. Bioassay-guided isolation and structure elucidation of the active extract (5.0 g) afforded 18 new 2,5-disubstituted lipophilic pyrroles (**4**−**21**) and eight previously reported analogues (**22**−**29**).[34−36] Compound **4** was isolated as an amorphous powder, and its molecular formula, $C_{29}H_{46}N_2O$, was established by HRESIMS. The presence of a disubstituted pyrrole nucleus was deduced from the ^{1}H NMR resonances (Table 1) at $\delta$ 9.38 (br s, 1H, N-H), 6.89 (dd, 1H, $J =$ 3.8, 2.8 Hz, H-3), and 6.11 (dd, 1H, $J =$ 3.8, 2.8 Hz, H-4) and the ^{13}C NMR resonances (Table 4) at $\delta$ 142.3 (C), 132.2 (C) 122.5 (CH), and 109.8 (CH). The 3.8 Hz coupling constant between the pyrrole protons, a typical value for $J_{3,4}$ in pyrroles,[36] indicated a 2,5-disubstitution pattern. A singlet resonance in the ^{1}H NMR spectrum ($\delta$ 9.39, s, 1H, H-1) together with a methine ^{13}C resonance at $\delta$ 178.4 (CH) was attributed to a formyl group conjugated to the pyrrole nucleus. The IR bands at 3260 and 1635 cm$^{-1}$ and UV absorption maxima at 301 nm ($\varepsilon$ 16 200) were characteristic of the pyrrole-2-carbaldehyde. Analysis of the HMQC spectrum indicated that four ^{1}H NMR multiplet resonances at $\delta$ 5.47 (m, 1H), 5.42 (m, 1H), 5.38 (m, 1H), and 5.28 (m, 1H) were coupled to the ^{13}C NMR resonances at $\delta$ 130.3 (CH), 128.1 (CH), 130.9 (CH), and 127.4 (CH), respectively. These were assigned to the olefinic protons of a 1,4-diene spin system on the basis of observation of [1]H−^{1}H COSY correlations (i.e., H-8/H-9/H$_2$-10/H-11/H-12). Furthermore, it was readily inferred that the double bonds were separated by a bis-allylic methylene moiety upon observation of the NMR resonances at $\delta_H$ 2.74 (m, 2H, H-10) and $\delta_C$ 25.8 (CH$_2$), and the chemical shift of the carbon resonance was typical of a ($Z,Z$)-1,4-disubstituted pattern of unsaturation.[37] The location of the olefinic system was determined from the 2D NMR spectra, which exhibited [1]H−^{1}H COSY correlations from H$_2$-7 ($\delta_H$ 2.44) to H$_2$-6 ($\delta_H$ 2.737) and H-8, as well as HMBC correlations between H$_2$-6 and C-7 ($\delta_C$ 26.9) and C-8 and between H$_2$-7 and C-5, C-6 ($\delta_C$ 28.1), C-8, and C-9. As in the structures of the previously reported *Mycale* metabolites mycalenitrile-1 (**22**) and mycaleni-trile-2 (**24**),[34] **4** also possessed a terminal nitrile moiety at $\delta$ 120.0 (C). The molecular formula and the presence of a nitrile carbon indicated that the olefinic system had to be connected to the nitrile

group through a sequence of 16 methylene carbons. Therefore, **4** was deduced to be a new nitrile-substituted 2,5-disubstituted pyrrole and was assigned the trivial name mycalenitrile-4.

Compound **5** was obtained as a viscous liquid that had the same $C_{29}H_{46}N_2O$ molecular formula (determined by HRESIMS on the quasi-molecular ion peak [M + Na]$^+$ at $m/z$ 461.3506) as **4**. The ^{1}H and ^{13}C NMR spectra (Tables 1 and 4) of **5** were very similar to those of **4**, except for modest differences in the chemical shifts of several resonances. Further comparison of the NMR spectra of **5** and **4** revealed that the only difference between them was the position of the olefinic system. This gave rise to ^{1}H NMR resonances in **5** at $\delta$ 5.37 (m, 4H) due to four olefinic protons, resonances at 2.10 (dt, 2H, $J =$ 7.2, 6.4 Hz, H-25) and 2.05 (dt, 2H, $J =$ 7.2, 6.8 Hz, H-19) that were attributable to two allylic methylenes, and a resonance at 2.78 (dd, 2H, $J =$ 6.4, 5.2 Hz, H-22) assignable to a bis-allylic methylene. The location of the olefinic system in the chain was deduced from analysis of the HMBC spectrum. In particular, the H$_2$-28 [$\delta$ 2.34 (t, 2H, $J =$ 7.2 Hz)] resonance showed diagnostic long-range correlations with the C-26 ($\delta$ 28.9) and C-27 ($\delta$ 25.6) methylene carbons, and the C-27 resonance, in turn, was coupled to the H$_2$-25 (2.10) allylic protons. Observation of the spin system from H$_2$-24 to H$_2$-28 in the [1]H−^{1}H COSY spectrum confirmed the position of the olefinic system. It was therefore concluded that the diene system was at the $\omega$-6 position,[34,37] and this related compound was deduced to be another nitrile-substituted 2,5-disubstituted pyrrole, which was named mycalenitrile-5 (**5**).

Compounds **6** and **7** were isolated as colorless oils. The HRESIMS indicated the molecular formulas $C_{25}H_{38}N_2O$ and $C_{27}H_{42}N_2O$ for each, respectively. Both compounds displayed NMR spectra that were nearly identical to those described for **5**, which suggested that **6** and **7** were also pyrrole-2-carbaldehydes and that each contained a 1,4-diene side chain. Furthermore, the olefinic systems in **6** and **7** were also deduced to be at $\omega$-6, following the same rationale described above for **5**. The molecular formulas of **6** and **7** indicated that the side chains in each were shortened by either four or two methylene units, respectively, and that the site of chain truncation was between the pyrrole ring and the 1,4-diene system (relative to the structure of **5**). Therefore, mycalenitrile-6 (**6**) and mycalenitrile-7 (**7**) were deduced to be the new nitrile-substituted lipophilic pyrroles.

Compound **8** was obtained as a white solid. The molecular formula $C_{25}H_{40}N_2O$ was determined by HRESIMS and from analysis of the ^{13}C NMR and DEPT spectra. Similarities in the spectroscopic data indicated that **8** was structurally similar to **6**. Analysis of the ^{1}H and ^{13}C NMR spectra of **8** indicated that the linear side chain of **8** contained only a single double bond [$\delta_H$ 5.36 (m, 2H); $\delta_C$ 130.4 (CH) and 129.6 (CH)]. The position of the double bond was determined by examination of the GC-EIMS fragmentation pattern. In particular, compound **8** afforded a molecular ion peak at $m/z$ 384 [M$^+$] and two ions at $m/z$ 234 and 288 due to fragments produced by allylic cleavage of the side chain.[36,38] The ion at $m/z$ 234 was due to the fragment containing the pyrrole nucleus ($C_{15}H_{24}NO^+$), while the ion at $m/z$ 288 arose from the fragment containing the pyrrole moiety and the olefin ($C_{19}H_{30}NO^+$). These data established that the double bond was located at C-17/ C-18 ($\omega$-8). Thus, mycalenitrile-8 (**8**) was deduced to be a new $\omega$-8 unsaturated lipophilic pyrrole.

Compounds **9** and **10** were isolated as a colorless oil and a white solid, respectively. Each possessed IR, UV, and NMR spectra that were nearly superimposable with those of **8**, indicating that the only differences between these structures was in the length of the lipophilic chain and position of the double bond. The molecular formulas of **9** ($C_{27}H_{44}N_2O$) and **10** ($C_{29}H_{48}N_2O$), deduced from the HRESIMS data, indicated that the side chain of each compound was elongated by either two or four methylenes, respectively, with respect to the structure of **8**. Compounds **9** and **10** exhibited a

**Table 1.** $^1$H NMR Data$^a$ $\delta$ (*J*, Hz) for **4**, **5**, **7**, and **10**−**12**

| H | 4 | 5 | 7 | 10 | 11 | 12 |
|---|---|---|---|---|---|---|
| 1 | 9.39, s | 9.37, s | 9.37, s | 9.36, s | 9.35, s | 9.38, s |
| 3 | 6.89, dd (3.8, 2.8) | 6.90, dd (3.6, 2.8) | 6.90, dd (3.6, 2.8) | 6.90, dd (3.2, 2.8) | 6.91, dd (3.2, 2.8) | 6.89, dd (3.6, 2.4) |
| 4 | 6.11, dd (3.8, 2.8) | 6.09, dd (3.6, 2.8) | 6.08, dd (3.6, 2.8) | 6.08, dd (3.2, 2.8) | 6.08, dd (3.2, 2.8) | 6.08, dd (3.6, 2.4) |
| 6 | 2.74, m | 2.67, t (7.6) | 2.68, t (7.6) | 2.68, t (7.2) | 2.68, t (7.2) | 2.66, t (7.6) |
| 7 | 2.44, dd (7.2, 6.8) | 1.68, m | 1.68, m | 1.66, m | 1.65, m | 1.66, m |
| 8 | 5.42, m | 1.27, br s | 1.27, br s | 1.26, br s | 1.26, br s | 1.27, br s |
| 9 | 5.47, m | 1.27, br s | 1.27, br s | 1.26, br s | 1.26, br s | 1.27, br s |
| 10 | 2.74, m | 1.27, br s | 1.27, br s | 1.26, br s | 1.36, m | 1.37, m |
| 11 | 5.28, m | 1.27, br s | 1.27, br s | 1.26, br s | 2.01, m | 2.01, m |
| 12 | 5.38, m | 1.27, br s | 1.27, br s | 1.26, br s | 5.34, m | 5.36, m |
| 13 | 2.02, dd (6.8, 6.6) | 1.27, br s | 1.27, br s | 1.26, br s | 5.34, m | 5.36, m |
| 14 | 1.26, br s | 1.27, br s | 1.27, br s | 1.26, br s | 2.01, m | 2.02, m |
| 15 | 1.26, br s | 1.27, br s | 1.27, br s | 1.26, br s | 1.36, m | 1.37, m |
| 16 | 1.26, br s | 1.27, br s | 1.27, br s | 1.26, br s | 1.26, br s | 1.27, br s |
| 17 | 1.26, br s | 1.27, br s | 2.04, dt (7.2, 6.4) | 1.26, br s | 1.26, br s | 1.27, br s |
| 18 | 1.26, br s | 1.27, br s | 5.37, m | 1.26, br s | 1.26, br s | 1.27, br s |
| 19 | 1.26, br s | 2.05, dt (7.2, 6.8) | 5.37, m | 1.38, m | 1.26, br s | 1.27, br s |
| 20 | 1.26, br s | 5.37, m | 2.78, t (6.0) | 2.02, m | 1.26, br s | 1.27, br s |
| 21 | 1.26, br s | 5.37, m | 5.37, m | 5.36, m | 1.26, br s | 1.27, br s |
| 22 | 1.26, br s | 2.78, dd (6.4, 5.2) | 5.37, m | 5.36, m | 1.26, br s | 1.27, br s |
| 23 | 1.26, br s | 5.37, m | 2.10, dt (7.2, 5.6) | 2.02, m | 1.26, br s | 1.27, br s |
| 24 | 1.26, br s | 5.37, m | 1.44, m | 1.38, m | 1.43, m | 1.27, br s |
| 25 | 1.26, br s | 2.10, dt (7.2, 6.4) | 1.66, m | 1.26, br s | 1.65, m | 1.43, m |
| 26 | 1.45, m | 1.44, m | 2.33, m | 1.44, m | 2.34, t (7.2) | 1.66, m |
| 27 | 1.67, m | 1.66, m | | 1.66, m | | 2.34, t (7.2) |
| 28 | 2.34, t (7.2) | 2.34, t (7.2) | | 2.35, t (6.8) | | |
| NH | 9.38, br s | 9.52, br s | 9.51, br s | 10.2, br s | 10.43, br s | 9.23, br s |

$^a$ Bruker AMX 400 MHz spectrometer; chemical shifts (ppm) referenced to CDCl$_3$ ($\delta_H$ 7.27); numerical order groups compounds of similar chain length.

**Table 2.** $^1$H NMR Data$^a$ $\delta$ (*J*, Hz) for **6**, **8**, **9**, and **19**−**21**

| H | 6 | 8 | 9 | 19 | 20 | 21 |
|---|---|---|---|---|---|---|
| 1 | 9.38, s | 9.37, s | 9.38, s | 9.38, s | 9.38, s | 9.37, s |
| 3 | 6.89, dd (2.4, 1.6) | 6.90, dd (3.7, 2.6) | 6.89, dd (3.2, 2.8) | 6.90, dd (3.6, 24) | 6.89, dd (3.6, 2.4) | 6.90, dd (3.2, 2.8) |
| 4 | 6.09, br s | 6.08, dd (3.7, 2.6) | 6.08, dd (3.2, 2.8) | 6.08, dd (3.6, 2.4) | 6.08, dd (3.2, 2.4) | 6.08, dd (3.2, 2.8) |
| 6 | 2.67, t (7.6) | 2.67, t (7.6) | 2.66, t (7.6) | 2.67, t (7.6) | 2.65, t (7.6) | 2.65, t (7.6) |
| 7 | 1.70, m | 1.66, m | 1.66, m | 1.66, m | 1.65, m | 1.65, br s |
| 8 | 1.26, br s | 1.27, br s | 1.27, br s | 1.27, br s | 1.27, br s | 1.27, br s |
| 9 | 1.26, br s | 1.27, br s | 1.27, br s | 1.27, br s | 1.27, br s | 1.27, br s |
| 10 | 1.26, br s | 1.27, br s | 1.27, br s | 1.27, br s | 1.27, br s | 1.27, br s |
| 11 | 1.26, br s | 1.27, br s | 1.27, br s | 1.27, br s | 1.27, br s | 1.27, br s |
| 12 | 1.26, br s | 1.27, br s | 1.27, br s | 1.27, br s | 2.09, m | 1.27, br s |
| 13 | 1.26, br s | 1.27, br s | 1.27, br s | 1.27, br s | 5.37, m | 1.27, br s |
| 14 | 1.26, br s | 1.27, br s | 1.27, br s | 2.06, m | 5.37, m | 2.08, m |
| 15 | 2.05, dt (6.8, 6.4) | 1.27, m | 1.27, br s | 5.37, m | 2.82, m | 5.37, m |
| 16 | 5.37, m | 2.02, m | 1.27, br s | 5.37, m | 5.37, m | 5.37, m |
| 17 | 5.37, m | 5.36, m | 1.38, m | 2.78, t (6.0) | 5.37, m | 2.82, m |
| 18 | 2.78, dd (6.0, 5.6) | 5.36, m | 2.03, m | 5.37, m | 2.82, m | 5.37, m |
| 19 | 5.37, m | 2.02, m | 5.35, m | 5.37, m | 5.37, m | 5.37, m |
| 20 | 5.37, m | 1.27, m | 5.35, m | 2.06, m | 5.37, m | 2.82, m |
| 21 | 2.11, dt (6.8, 6.0) | 1.27, br s | 2.03, m | 1.43, dq (7.2, 6.0) | 2.09, m | 5.37, m |
| 22 | 1.44, m | 1.44, m | 1.38, m | 0.92, t (7.2) | 0.98, t (7.6) | 5.37, m |
| 23 | 1.65, m | 1.66, m | 1.27, br s | | | 2.08, m |
| 24 | 2.34, m | 2.34, t (6.8) | 1.45, m | | | 0.99, t (7.6) |
| 25 | | | 1.66, m | | | |
| 26 | | | 2.34, t (7.2) | | | |
| NH | 9.22, br s | 9.71, br s | 9.24, br s | 9.47, br s | 9.16, br s | 9.29, br s |

$^a$ Bruker AMX 400 MHz spectrometer; chemical shifts (ppm) referenced to CDCl$_3$ ($\delta_H$ 7.27); numerical order groups compounds of similar chain length.

similar GC-EIMS cleavage pattern to that observed with **8**. Specifically, each produced the fragment ions (*m/z* 262 and 316 for **9**; *m/z* 290 and 344 for **10**), with a difference of 54 mass units. These data suggested that the side-chain olefinic bond in each compound was also at the $\omega$-8 position. Consequently, mycaleni-trile-9 (**9**) and mycalenitrile-10 (**10**) were deduced to be two new lipophilic nitrile-substituted pyroles that each contained a single double bond in their respective side chains at the $\omega$-8 position.

Compounds **11** and **12** were obtained as colorless oils of molecular formulas C$_{27}$H$_{44}$N$_2$O and C$_{28}$H$_{46}$N$_2$O, respectively (as deduced from analysis of the HRESIMS data). This suggested that each compound differed only by the presence of one methylene

group. As in the structures of **8**−**10**, the 1D NMR data (Tables 1 and 4) of **11** and **12** revealed that the side chains in each compound contained only a single double bond. The loss of 54 mass units between the fragment ions at *m/z* 164 and 218 in the GC-EIMS of each compound indicated that the double bonds in each were located at the C-12 position. Therefore, mycalenitrile-11 (**11**) and my-calenitrile-12 (**12**) were deduced to be two new lipophilic pyroles.

Compound **13** was obtained as a yellow solid. Its molecular formula, C$_{21}$H$_{34}$N$_2$O, was established by HRESIMS. The presence of the pyrrole-2-carbaldehyde nucleus was confirmed upon observa-tion of the NMR resonances at $\delta_H$ 9.48 (br s, 1H, N-H), 9.37 (s, 1H, H-1), 6.90 (dd, 1H, *J* = 3.8, 2.8 Hz, H-3), and 6.08 (dd, 1H,

**Table 3.** $^1H$ NMR Data$^a$ $\delta$ ($J$, Hz) for **13−18**

| H | 13 | 14 | 15 | 16 | 17 | 18 |
|---|----|----|----|----|----|----|
| 1 | 9.37, s | 9.38, s | 9.37, s | 9.35, s | 9.38, s | 9.38, s |
| 3 | 6.90, dd (3.8, 2.8) | 6.89, br s | 6.90, dd (3.2, 2.8) | 6.90, dd (3.6, 2.8) | 6.88, dd (3.6, 2.8) | 6.89, dd (3.2, 2.8) |
| 4 | 6.08, dd (3.8, 2.8) | 6.08, br s | 6.08, dd (3.2, 2.8) | 6.09, dd (3.6, 2.8) | 6.08, dd (3.6, 2.8) | 6.08, dd (3.2, 2.8) |
| 6 | 2.66, t (7.6) | 2.66, t (7.6) | 2.66, t (7.6) | 2.66, t (7.6) | 2.71, t (7.6) | 2.66, t (7.6) |
| 7 | 1.66, m | 1.66, m | 1.66, m | 1.67, m | 2.41, t (7.2) | |
| 8 | 1.26, br s | 1.27, br s | 1.27, br s | 1.29, br s | 5.39, m | 1.27, br s |
| 9 | 1.26, br s | 1.27, br s | 1.27, br s | 1.29, br s | 5.46, m | 1.27, br s |
| 10 | 1.26, br s | 1.27, br s | 1.27, br s | 1.29, br s | 2.01, m | 1.27, br s |
| 11 | 1.26, br s | 1.27, br s | 1.27, br s | 1.29, br s | 1.26, br s | 2.03, m |
| 12 | 1.26, br s | 1.27, br s | 1.27, br s | 1.29, br s | 1.26, br s | 5.37, m |
| 13 | 1.26, br s | 1.27, br s | 1.27, br s | 1.29, br s | 1.26, br s | 5.37, m |
| 14 | 1.26, br s | 1.27, br s | 1.27, br s | 2.03, m | 1.26, br s | 2.03, m |
| 15 | 1.26, br s | 1.27, br s | 1.27, br s | 5.37, m | 1.26, br s | 1.27, br s |
| 16 | 1.26, br s | 1.27, br s | 1.27, br s | 5.37, m | 1.26, br s | 1.27, br s |
| 17 | 1.26, br s | 1.27, br s | 1.27, br s | 2.03, m | 1.26, br s | 1.27, br s |
| 18 | 1.45, m | 1.27, br s | 1.27, br s | 1.29, br s | 1.26, br s | 1.27, br s |
| 19 | 1.66, m | 1.27, br s | 0.89, t (6.4) | 1.29, br s | 1.67, m | 1.67, m |
| 20 | 2.34, t (7.2) | 1.27, br s | | 1.29, br s | 0.86, d (7.6) | 0.87, d (7.6) |
| 21 | | 1.45, m | | 1.29, br s | 0.86, d (7.6) | 0.87, d (7.6) |
| 22 | | 1.66, m | | 0.89, t (7.2) | | |
| 23 | | 2.34, t (7.2) | | | | |
| NH | 9.48, br s | 9.49, br s | 9.44, br s | 9.25, br s | 9.17, br s | 9.16, br s |

$^a$ Bruker AMX 400 MHz spectrometer; chemical shifts (ppm) referenced to CDCl$_3$ ($\delta_H$ 7.27); numerical order groups compounds of similar chain length.

**Table 4.** $^{13}C$ NMR Data$^a$ ($\delta$, DEPT) for **4**, **5**, **7**, and **10−12**

| C | 4 | 5 | 7 | 10 | 11 | 12 |
|---|----|----|----|----|----|----|
| 1 | 178.4, CH | 178.3, CH | 178.3, CH | 178.2, CH | 178.3, CH | 178.3, CH |
| 2 | 132.2, C | 132.1, C | 132.1, C | 132.0, C | 132.1, C | 132.0, C |
| 3 | 122.5, CH | 122.6, CH | 122.7, CH | 122.7, CH | 122.8, CH | 122.7, CH |
| 4 | 109.8, CH | 109.7, CH | 109.7, CH | 109.6, CH | 109.6, CH | 109.7, CH |
| 5 | 142.3, qC | 142.8, C | 143.0, C | 143.4, C | 143.4, C | 142.9, C |
| 6 | 28.1, CH$_2$ | 28.0, CH$_2$ | 28.0, CH$_2$ | 28.0, CH$_2$ | 28.1, CH$_2$ | 28.1, CH$_2$ |
| 7 | 26.9, CH$_2$ | 28.7, CH$_2$ | 28.7, CH$_2$ | 28.9, CH$_2$ | 29.0, CH$_2$ | 29.0, CH$_2$ |
| 8 | 128.1, CH | 29.9−29.0$^b$ | 29.9−29.0$^b$ | 29.9−29.4$^b$ | 29.9−29.4 | 30.0−29.5$^b$ |
| 9 | 130.3, CH | 29.9−29.0$^b$ | 29.9−29.0$^b$ | 29.9−29.4$^b$ | 29.9−29.4 | 30.0−29.5$^b$ |
| 10 | 25.8, CH$_2$ | 29.9−29.0$^b$ | 29.9−29.0$^b$ | 29.9−29.4$^b$ | 29.2, CH$_2^c$ | 29.1, CH$_2$ |
| 11 | 127.4, CH | 29.9−29.0$^b$ | 29.9−29.0$^b$ | 29.9−29.4$^b$ | 27.4, CH$_2^c$ | 27.5, CH$_2^c$ |
| 12 | 130.9, CH | 29.9−29.0$^b$ | 29.9−29.0$^b$ | 29.9−29.4$^b$ | 130.4, CH$^d$ | 130.5, CH$^{dc}$ |
| 13 | 27.4, CH$_2$ | 29.9−29.0$^b$ | 29.9−29.0$^b$ | 29.9−29.4$^b$ | 129.6, CH$^d$ | 129.6, CH$^d$ |
| 14 | 29.9−29.0$^b$ | 29.9−29.0$^b$ | 29.9−29.0$^b$ | 29.9−29.4$^b$ | 27.2, CH$_2^e$ | 27.2, CH$_2^c$ |
| 15 | 29.9−29.0$^b$ | 29.9−29.0$^b$ | 29.9−29.0$^b$ | 29.9−29.4$^b$ | 29.1, CH$_2^c$ | 29.1, CH$_2$ |
| 16 | 29.9−29.0$^b$ | 29.9−29.0$^b$ | 29.9−29.0$^b$ | 29.9−29.4$^b$ | 29.9−29.4$^b$ | 30.0−29.5$^b$ |
| 17 | 29.9−29.0$^b$ | 29.9−29.0$^b$ | 27.5, CH$_2$ | 29.9−29.4$^b$ | 29.9−29.4$^b$ | 30.0−29.5$^b$ |
| 18 | 29.9−29.0$^b$ | 29.9−29.0$^b$ | 128.0, CH | 29.9−29.4$^b$ | 29.9−29.4$^b$ | 30.0−29.5$^b$ |
| 19 | 29.9−29.0$^b$ | 27.5, CH$_2$ | 130.6, CH | 29.2, CH$_2^e$ | 29.9−29.4$^b$ | 30.0−29.5$^b$ |
| 20 | 29.9−29.0$^b$ | 127.9, CH | 25.9, CH$_2$ | 27.4, CH$_2^{c-e}$ | 29.9−29.4$^b$ | 30.0−29.5$^b$ |
| 21 | 29.9−29.0$^b$ | 130.6, CH | 128.9, CH | 130.3, CH$^d$ | 29.9−29.4$^b$ | 30.0−29.5$^b$ |
| 22 | 29.9−29.0$^b$ | 25.9, CH$_2$ | 129.6, CH | 129.6, CH$^d$ | 29.9−29.4$^b$ | 30.0−29.5$^b$ |
| 23 | 29.9−29.0$^b$ | 128.9, CH | 27.0, CH$_2$ | 27.2, CH$_2^c$ | 29.9−29.4$^b$ | 30.0−29.5$^b$ |
| 24 | 29.9−29.0$^b$ | 129.5, CH | 28.9, CH$_2$ | 29.1, CH$_2^e$ | 28.8, CH$_2$ | 30.0−29.5$^b$ |
| 25 | 29.9−29.0$^b$ | 27.0, CH$_2$ | 25.6, CH$_2$ | 29.9−29.4 | 25.6, CH$_2$ | 28.9, CH$_2$ |
| 26 | 28.9, CH$_2$ | 28.9, CH$_2$ | 17.3, CH$_2$ | 28.8, CH$_2$ | 17.3, CH$_2$ | 25.6, CH$_2$ |
| 27 | 25.6, CH$_2$ | 25.6, CH$_2$ | 120.1, C | 25.5, CH$_2$ | 120.0, C | 17.4, CH$_2$ |
| 28 | 17.3, CH$_2$ | 17.3, CH$_2$ | | 17.3, CH$_2$ | | 120.1, C |
| 29 | 120.0, C | 120.1, C | | 120.0, C | | |

$^a$ Bruker AMX 100 MHz spectrometer; $\delta$ values are reported in ppm referenced to CDCl$_3$ ($\delta_C$ 77.23) as internal standard; numerical order groups compounds of similar chain length; $^b$ All carbons were CH$_2$. $^{c-e}$ Values may be interchanged.

$J$ = 3.8, 2.8 Hz, H-4) and $\delta_C$ 178.3 (CH), 143.3 (C), 132.1 (C), 122.7 (CH), and 109.7 (CH). The remaining $^{13}C$ resonances were assignable to side-chain methylenes, with the exception of the $\delta$ 120.0 quaternary nitrile carbon, indicating that **13** possessed a fully saturated alkyl side chain. Thus, mycalenitrile-13 (**13**) was deduced to be a new lipophilic nitrile-substituted pyrrole with a saturated side chain.

Compound **14** was isolated as a white solid. The $^1H$ and $^{13}C$ NMR spectra of **14** were nearly identical to those of **13**, indicating that **14** was also a fully unsaturated pyrrole-2-carbaldehyde. The molecular formula $C_{24}H_{40}N_2O$ indicated the alkyl chain was elongated by three methylenes relative to the structure of **13**.

Therefore, this analogue of **13** with a longer side chain was assigned the trivial name mycalenitrile-14 (**14**).

Compound **15** was obtained as an amorphous powder with a molecular formula of $C_{19}H_{33}NO$, indicating the absence of one nitrogen atom in the structure, relative to the structures of **4−14**. The spectroscopic data of **15** were similar to those of **13** and **14**. Detailed analysis of NMR spectra established that **15** differed from **13** and **14** only by the terminal alkyl side-chain substituent (i.e., a terminal methyl group rather than the nitrile moiety in **13** and **14**). This methyl group gave rise to a new $^1H$ NMR resonance at $\delta$ 0.89 (t, 3H, $J$ = 6.4 Hz, H-19) and replacement of the downfield $\omega$-2 and $\omega$-3 methylene resonances (observed in **13** and **14**) with

only a broad second-order-coupled pattern of methylene resonances at $\delta$ 1.27 (br s, 22H, H-8 to H-18). Therefore, this new compound, mycalazal-14 (**15**), was deduced to be a new mycalazal-type 5-tetradecylpyrrole-2-carbaldehyde with a fully saturated lipophilic side chain.

Compound **16** was isolated as a colorless oil. The molecular formula $C_{22}H_{37}NO$ was deduced by HRESIMS on the sodiated molecular ion at $m/z$ 354.2748. The $^1H$ and $^{13}C$ NMR spectra indicated that, in addition to the 2,5-disubstituted pyrrole moiety and formyl group resonances, specific resonances were attributable to a linear monounsaturated alkyl side chain. In particular, the $^1H$ NMR spectrum of **16** exhibited two olefinic proton resonances at $\delta$ 5.37 (m, 2H), one terminal methyl triplet at $\delta$ 0.89 (t, $H_3$, $J =$ 7.2 Hz), and one four-proton multiplet at $\delta$ 2.03 (4H, H-14 and H-17) due to two allylic methylenes that were correlated in the HSQC spectrum with carbon resonances at $\delta$ 27.4 (2C). These data suggested that compound **16** contained a $C_{17}$ hydrocarbon side chain with one double bond with *Z*-geometry. The $\Delta^{15}$ position of the olefinic bond was determined from the GC-EIMS, which contained fragment ions at $m/z$ 206 and 260, which resulted from allylic cleavage of the side-chain olefin. Thus, the structure of mycalazal-15 (**16**) was deduced to be a new lipophilic pyrrole with a single double bond in the lipophilic side chain at the $\omega$-7 position.

Compound **17** was isolated as a colorless oil. The HRESIMS showed a quasi-molecular ion peak at $m/z$ 340.2641 [M + Na]$^+$, corresponding to the molecular formula $C_{21}H_{35}NONa$, which required five degrees of unsaturation. The $^1H$ and $^{13}C$ NMR spectra of **17** were similar to those of **16**, except for the absence of the methyl triplet (0.89 in **16**), which was replaced by an isopropyl methyl doublet at $\delta$ 0.86 (d, $J =$ 7.6 Hz) that integrated for six protons. Thus, the pyrrole-2-carbaldehyde moiety was substituted at C-5 with a monounsaturated hydrocarbon side chain with a terminal isopropyl group. The position of the double bond was assigned at C-8 by $^1H-^1H$ COSY correlations that established the H-6 to H-8 spin system. Therefore, the structure of this new *Mycale* metabolite mycalazal-16 (**17**) was deduced to be a mycalazal-type lipophic pyrrole-2-carbaldehyde with a branched side chain.

Compound **18** was isolated as a colorless oil. It was isomeric with **17**, having a molecular formula of $C_{21}H_{35}NO$ as determined by the HRESIMS. However, the NMR spectra of these two compounds were distinctly different. In particular, the $^1H$ NMR spectrum of **18** exhibited both olefinic proton resonances as a single multiplet resonance centered at $\delta$ 5.37 (2H), rather than as two distinct signals at $\delta$ 5.39 and 5.46, as observed in **17**. In addition, the presence of an additional higher field allylic methylene resonance at $\delta$ 2.03 (m) indicated that the difference between **18** and **17** was in the location of the olefinic bond. The position of the double bond in **18** was deduced to be at C-12 by observation of the allylic cleavage fragmentation ions at $m/z$ 164 and 218 in the GC-EIMS spectrum. On the basis of these data and the molecular formula, **18** was deduced to possess a $\Delta^7$-14-methylpentadecenyl side chain. Therefore, mycalazal-17 (**18**) was deduced to be an $\omega$-8 unsaturated isomer of **17**.

Compound **19** was obtained as a colorless oil and showed a HRESIMS quasi-molecular ion [M + Na]$^+$ at $m/z$ 352.2621, compatible with the molecular formula $C_{22}H_{35}NONa$. The $^1H$ NMR spectrum contained the typical H-3, H-4, and N-H resonances of the pyrrole nucleus. Because the pyrrole-2-carbaldehyde moiety accounted for five carbons, four degrees of unsaturations, and all the heteroatoms of the molecular formula, it was deduced that compound **19** contained a $C_{17}$ hydrocarbon side chain with two double bonds. Furthermore, it was evident that the two double bonds were in a 1,4-diene pattern by the presence of bis-allylic methylene $^1H$ NMR resonances at $\delta$ 2.78 (t, 2H, $J =$ 6.0 Hz) and $\delta_C$ 25.9 (CH$_2$). The COSY $^1H-^1H$ spin systems identified the 15,18-diene functionality. Specifically, $^1H-^1H$ couplings were observed between H-19 ($\delta$ 5.37) and H$_2$-20 ($\delta$ 2.06), between H$_2$-21 ($\delta$ 1.43) and

H$_2$-20, and between H$_2$-21 and H$_3$-22 ($\delta$ 0.92). This was further confirmed by observation of long-range heteronuclear (HMBC) couplings from H$_3$-22 to C-21 ($\delta_C$ 23.0) and C-22 ($\delta_C$ 29.4). Thus, mycalazal-18 (**19**) was deduced to be a new pyrrole-2-carbaldehyde with a 1,4-diene in its lipophilic side chain.

Compound **20** was isolated as a colorless oil with a molecular formula of $C_{22}H_{33}NO$. This formula required one more degree of unsaturation relative to the structure of **19**. This indicated that **20** was a pyrrole-2-carbaldehyde analogue with one additional double bond in the hydrocarbon side chain. This structural assignment of **20** was further confirmed by a $^1H$ NMR multiplet at $\delta$ 5.37 that integrated for six olefinic protons and six $^{13}C$ NMR sp$^2$ methine resonances at $\delta$ 132.0, 130.4, 128.5, 128.4, 128.0, and 127.3, which were attributable to three disubstituted double bonds. These data, together with two $^1H$ NMR multiplets at $\delta$ 2.82 (4H) and 2.09 (4H) assignable to two bis-allylic methylenes and two allylic methylenes, respectively, were in agreement with a sequence of three methylene-interrupted double bonds (1,4,7-unsaturation pattern). Further, the combined analysis of the 1D and 2D NMR spectra indicated that the olefinic system in **20** was at the $\omega$-3 position on the basis of the $^1H-^1H$ COSY correlation between the terminal methyl resonance at H$_3$-22 [$\delta$ 0.98 (t, $J =$ 7.6 Hz)] and the allylic methylene H$_2$-21 ($\delta$ 2.09) resonance. This was further supported by long-range HMBC correlations from the H$_3$-22 terminal methyl resonance to the C-20 ($\delta$ 132.0) olefinic carbon and the chemical shift of one of the $\omega$-2 allylic methylene resonances at $\delta$ 20.8. Thus, the structure of this *Mycale* metabolite, mycalazal-19 (**20**), was deduced to be a pyrrole-2-carbaldehyde with a 1,4,7-triene at the $\omega$-3 position in the lipophilic side chain.

Compound **21** was isolated as a colorless oil. It exhibited IR, UV, and NMR spectra nearly identical to those of **20**, indicating that the two compounds differed only in side-chain length. The molecular formula of $C_{24}H_{37}NO$ indicated that **21** contained a side chain elongated by two methylene units between the pyrrole ring and the olefinic system, relative to the structure of **20**. Therefore, mycalazal-20 (**21**) was deduced to be an analogue of **20** with a longer side chain.

The structures of **22–29** were readily identified by comparison of the spectroscopic and mass spectrometric data with those reported in the literature. The structures were identified as mycalenitrile-1 (**22**),[34] a pyrrole-2-carbaldehyde with a nitrile-substituted saturated lipophilic side chain (**23**),[35] mycalenitrile-2 (**24**),[34] 5-pentadecylpyrrole-2-carbaldehyde (**25**),[36] 5-hexadecylpyrrole-2-carbaldehyde (**26**),[36] a mycalazal-type lipophic pyrrole-2-carbaldehyde with a saturated side chain that contained a terminal isopropyl group (**27**),[35] an analogue of **27** with a longer side chain (**28**),[35] and mycalazal-3 (**29**).[34]

Previous reports have indicated that certain *M. cecilia* mycalazals (structurally related to **15–17** and **29**) and mycalenitriles (structurally related to **12** and **13**) suppress tumor cell viability (IC$_{50}$ values range from approximately 5 to 15 $\mu$M).[34] However, the mechanisms responsible for these observed antiproliferative effects are not known. Using the T47D cell-based HIF-1 activation reporter assay, 26 of the structurally related mycalazal/mycalenitrile-like metabolites (**4–29**) were titrated to determine their effects on HIF-1 activation.[23–25] On the basis of their HIF inhibitory activities, these compounds are divided into four groups. The most active compounds (**6** and **7**) inhibited hypoxia-induced HIF-1 activation with IC$_{50}$ values of 7.8 $\mu$M (95% confidence intervals: 6.8 to 8.8 $\mu$M) and 8.6 $\mu$M (95% confidence intervals: 7.6 to 9.9 $\mu$M), respectively (Figure 1A). The moderately active group (**5**, **8**, **13**, and **22**) exhibited IC$_{50}$ values between 10 and 20 $\mu$M (Figure 1B). The IC$_{50}$ values for the weakly active group (**15**, **17–19**, **21**, **27**, and **29**) ranged from 20 to 30 $\mu$M. The remaining 13 compounds (**4**, **9–12**, **14**, **16**, **20**, **23–26**, and **28**) did not significantly suppress hypoxia (1% O$_2$)-induced HIF-1 activation (<50% inhibition at 30 $\mu$M, the highest concentration tested). In comparison to their inhibitory
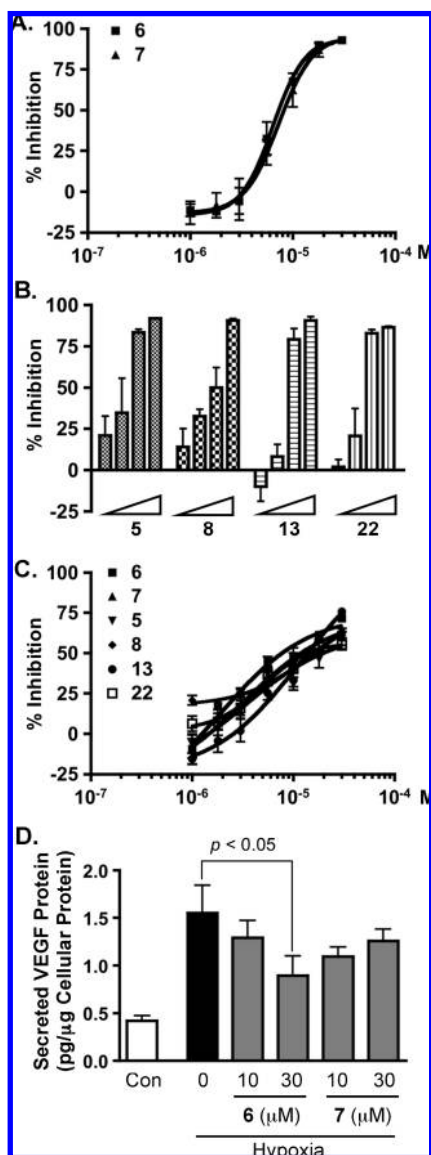
**Figure 1.** Inhibition of HIF-1 activation. (A) Concentration-dependent inhibitory effects exerted by **6** and **7** on hypoxia (1% $O_2$)-induced HIF-1 activation in a T47D cell-based reporter assay (mean ± SD, one experiment in triplicate). (B) Compounds **5**, **8**, **13**, and **22** were evaluated at 5.6, 10, 17.8, and 30 $\mu M$ in the reporter assay described in (A). (C) Concentration−response results of **5**−**8**, **13**, and **22** on 1,10-phenanthroline (10 $\mu M$)-induced HIF-1 activation in a T47D cell-based reporter assay (mean ± SD, one experiment in triplicate). (D) Levels of secreted VEGF protein in the media conditioned by T47D cells exposed to hypoxia in the presence of **6** or **7** (1% $O_2$, 16 h) were determined by ELISA and normalized to the amounts of cellular proteins (mean ± SD, one experiment in triplicate). The *p* value was provided when there was a statistically significant difference between the hypoxia-induced and the compound-treated samples.

effects on hypoxia-induced HIF-1 activation, compounds from both the most active and the moderately active groups had less effect on chemical hypoxia-induced HIF-1 activation (1,10-phenanthroline at 10 $\mu M$, Figure 1C). One of the well-studied HIF-1 target genes is vascular endothelial growth factor (VEGF), an angiogenic factor that is critical for tumor angiogenesis.[39] Agents that inhibit VEGF are in clinical use for the treatment of cancer. The effects of **6** and **7** on hypoxia-stimulated production of secreted VEGF proteins were examined in T47D cells (Figure 1D). Compound **6** inhibited the hypoxia-induced increase in the level of secreted VEGF proteins by 50% at the concentration of 30 $\mu M$, while **7** did not significantly

inhibit secreted VEGF levels at the concentrations tested (10 and 30 $\mu M$). As observed in previous studies, significantly higher concentrations of HIF-1 inhibitors are required to inhibit the induction of VEGF expression, relative to the concentrations that inhibit HIF-1 activation in the cell-based reporter assay. The most potent HIF-1 inhibitory *Mycale* lipophilic pyrroles appear to possess the terminal nitrile functionality. These observations are in contrast to the SARs previously reported of LNCaP tumor cell cytotoxicity, where the nitrile-substituted mycalenitriles exhibited little or no significant activity and the $\omega$-7 monounsaturated (e.g., mycalazal-8) and $\omega$-3 triunsaturated mycalazals [e.g., mycalazal-3 (**29**)] were among the most cytotoxic.[34] As an inhibitor of hypoxia-induced HIF-1 activation, **29** showed only very weak activity. One thing to note is that Zubía and co-workers described significant SARs only related to LNCaP tumor cell cytotoxicity.[34] These previous studies also reported that the nitrile-substituted mycalenitriles displayed enhanced cytotoxic effects toward LoVo and HeLa cells. In our studies, few other structure−activity relationships were apparent. However, the SAR data were complicated by the highly lipophilic nature of these metabolites. It also appears that while a highly lipophilic alkyl side chain is essential for the HIF-1 inhibitory activity, extremely hydrophobic nonsubstituted long-chain analogues were nearly inactive. This may have resulted from the limited solubility of the most lipophilic compounds in the aqueous-based media used for the cell-based bioassays.

Compounds that disrupt the functioning of the mitochondrial electron transport chain (ETC) represent an important group of small-molecule HIF-1 inhibitors that are highly selective toward hypoxia-induced HIF-1 activation.[24,25,40,41] The observation that active compounds such as **6** and **7** demonstrated greater inhibitory activity toward hypoxia-induced HIF-1 activation, relative to their effects on chemical hypoxia/iron chelator-induced HIF-1 activation (Figure 1), and their highly lipophilic structures prompted us to test the hypothesis that these compounds may function as inhibitors of mitochondrial respiration. Concentration−response studies were performed to investigate the effects of **6** and **7** on T47D cell respiration (Figure 2A). Two structurally related, yet inactive, compounds, **10** and **24**, were included as negative controls. Compounds **6** and **7** inhibited T47D cell respiration in a concentration-dependent manner, and the concentrations that inhibited respiration correlated with those that inhibited hypoxia-induced HIF-1 activation in T47D cells ($IC_{50} < 10$ $\mu M$). As anticipated, compounds **10** and **24** did not exert significant inhibition of mitochondrial respiration ($IC_{50} > 30$ $\mu M$). Further mechanistic studies were conducted to discern the component(s) of the ETC that were affected by active compounds **6** and **7**. Substrates and/or inhibitors for each ETC complex were added in a sequential manner to permeabilized T47D cells. Addition of a mixture of malate and pyruvate initiated mitochondrial respiration at complex I (NADH-ubiquinone oxidoreductase). The complex I inhibitor rotenone suppressed this respiration, and the complex II substrate succinate overcame this inhibition (Figure 2B and C).[24,25] The observation that neither **6** nor **7** affected mitochondrial respiration in the presence of succinate indicated that **6** and **7** did not inhibit complex II, III, or IV (Figure 2B and C). Respiration in the presence of succinate was inhibited by the complex III inhibitor antimycin A, and respiration was reinitiated by addition of the complex IV substrates TMPD/ascorbate (Figure 2B and C). As observed in the case of mitochondrial complex I inhibitors (e.g., rotenone), the complex II substrate succinate re-established mitochondrial respiration following inhibition exerted by **6** and **7** (Figure 2D and E). Thus, the data presented in Figure 2 indicate that compounds **6** and **7** appear to selectively inhibit mitochondrial respiration at complex I.

Under hypoxic conditions, increased production of reactive oxygen species (ROS) by the $Q_o$ site of mitochondrial complex III may act as "signal molecules" of cellular hypoxia. The ROS appear
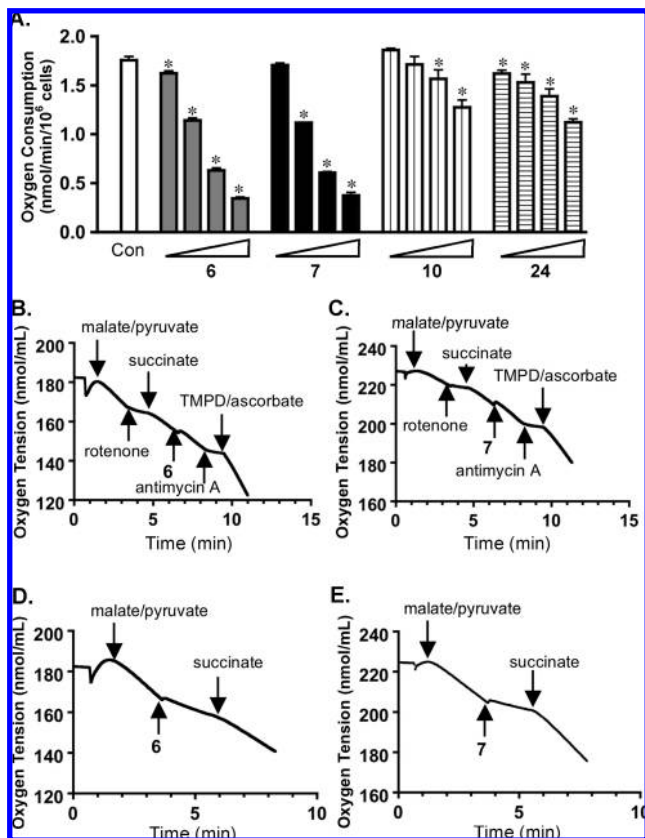
**Figure 2.** Compounds **6** and **7** inhibit mitochondrial respiration at complex I. (A) Concentration−response results of compounds **6**, **7**, **10**, and **24** on oxygen consumption by T47D cells (mean ± SD, three independent experiments). The compounds were tested at 1, 3, 10, and 30 $\mu$M. An asterisk (*) indicates statistically significant difference ($p < 0.05$) between the control and the compound-treated sample, compared by one-way ANOVA and Bonfferoni post hoc analyses (GraphPad Prism 4.0). (B) Compound **6** (10 $\mu$M) did not affect mitochondrial electron transport chain (ETC) complex II, III, or IV. Substrates and inhibitors were added to T47D cells (5 × 10$^6$, 30 °C) in a sequential manner at the specified time point. (C) Compound **7** (10 $\mu$M) did not affect ETC complex II, III, or IV. (D) Compound **6** (10 $\mu$M) suppressed mitochondria respiration by inhibiting complex I. (E) Compound **7** (10 $\mu$M) inhibited complex I.

to oxidize the catalytic iron in the Fe(II)-dependent HIF-prolyl hydroxylases that are required to "tag" HIF-1$\alpha$ protein for degradation by the proteasome.[42,43] Therefore, compounds that inhibit electron transport upstream from complex III, but do not themselves increase ROS production to the cytoplasmic site of the mitochondrial inner membrane at the site of inhibition, are able to prevent hypoxic mitochondria from releasing essential ROS signaling molecules needed to stabilize HIF-1$\alpha$ protein and activate HIF-mediated gene transcription.

## Experimental Section

**General Experimental Procedures.** Melting points were measured with a Thomas-Hoover capillary melting point apparatus and were uncorrected. A Bruker Tensor 27 Genesis Series FTIR was used to obtain the IR spectrum, and a Varian 50 Bio spectrophotometer was used to record the UV spectra. The NMR spectra were recorded in CDCl$_3$ on AMX-NMR spectrometers (Bruker) operating at 400 MHz for $^1$H and 100 MHz for $^{13}$C, respectively. Residual solvent peaks (7.27 for $^1$H and 77.23 for $^{13}$C) were used as internal references for the NMR spectra recorded running gradients. The HRESIMS spectra were determined on a Bruker Daltonic micro TOF fitted with an Agilent 1100 series HPLC and an electrospray ionization source. The GC-EIMS study was performed on a fused-silica DB5 capillary column (i.d. =

0.80 mm; film thickness = 0.15 $\mu$m; length = 32 m) and recorded on a Hewlett-Packard HP6980 Series gas chromatograph interfaced with a HP5973 mass selective detector at 70 eV. HPLC was performed on a Waters system, equipped with a 600 controller and a 996 photodiode array detector. Three semipreparative HPLC columns [(1) Phenomenex Luna RP-18, 5 $\mu$m, 250 × 10.00 mm; (2) Phenomenex Luna Si gel, 5 $\mu$m, 100 Å, 250 × 10.00 mm; and (3) Phenomenex Luna Phenyl-Hexyl, 5 $\mu$m, 100 Å, 250 × 10.00 mm] were employed for isolation. The TLCs were performed using Merck Si$_{60}$F$_{254}$ or Si$_{60}$RP$_{18}$F$_{254}$ plates, sprayed with a 10% H$_2$SO$_4$ solution in H$_2$O, heated, and visualized under UV at 254 nm.

**Sponge Material.** The extract was provided by the National Cancer Institute's Open Repository Program. *Mycale* (*Carmia*) sp. was collected at 12 m depth on July 5, 1993 (collection C011823), from Turtle Bas, Palau. The sample was identified by Dr. Michele Kelly (National Institute of Water and Atmospheric Research Limited, Auckland, New Zealand). The sponge material was frozen at −20 °C and ground in a meat grinder. A voucher specimen was placed on file with the Department of Invertebrate Zoology at the National Museum of Natural History located in Washington, DC.

**Extraction and Isolation.** Ground sponge material was extracted with H$_2$O. The residual sample was lyophilized and extracted with CH$_2$Cl$_2$/MeOH (1:1), residual solvents were removed under vacuum, and the extract was stored at −20 °C in the NCI repository at the Frederick Cancer Research and Development Center (Frederick, MD). The crude extract (5.0 g) inhibited hypoxia (1% O$_2$)-induced HIF-1 activation by 53% at 5 $\mu$g mL$^{-1}$ in a T47D cell-based reporter assay and was separated into four fractions by Sephadex LH-20 column chromatography [CHCl$_3$ in MeOH (1:1)] based on TLC analysis. The active fraction (4.4 g) inhibited hypoxia-induced HIF-1 activation by 50% at 5 $\mu$g mL$^{-1}$ and was further separated into five subfractions using a Sephadex LH-20 column eluted with petroleum ether/CHCl$_3$/MeOH at the ratio of 2:1:1. The active subfraction (3.7 g) inhibited hypoxia-induced HIF-1 activation by 48% at 5 $\mu$g mL$^{-1}$ and was subjected to C$_{18}$ VLC column chromatography (eluted with step gradients of 80% to 100% MeOH in H$_2$O), which gave rise to seven fractions. The second fraction (98.1 mg, eluted with 80% MeOH in H$_2$O) inhibited hypoxia-induced HIF-1 activation by 90% at 1 $\mu$g mL$^{-1}$ and was further separated by reversed-phase HPLC (Luna 5 $\mu$m, ODS-3 100 Å, 250 × 10.00 mm, isocratic 80% CH$_3$CN in H$_2$O, 4.0 mL min$^{-1}$) to produce **6** (0.9 mg, 0.02% yield, $t_R$ 29 min), **13** (3.0 mg, 0.06% yield, $t_R$ 18 min), and **22** (4.1 mg, 0.08% yield, $t_R$ 31 min). The third fraction (1.4 g, eluted with 90% MeOH in H$_2$O) inhibited hypoxia-induced HIF-1 activation by 56% at 5 $\mu$g mL$^{-1}$ and was further separated by semipreparative RP-HPLC eluting with isocratic 90% CH$_3$CN in H$_2$O, which afforded 11 subfractions. Further purification was achieved through repeated semipreparative HPLC with (1) Luna 5 $\mu$m, ODS-3 100 Å, 250 × 10.00 mm, isocratic solvents of various proportions of CH$_3$CN in H$_2$O, 4.0 mL min$^{-1}$; (2) Luna 5 $\mu$m, Si gel 100 Å, 250 × 10.00 mm, isocratic solvents of various proportions of 2-propanol in hexanes, 4.0 mL min$^{-1}$; and (3) Luna 5 $\mu$m, Phenyl-Hexyl 100 Å, 250 × 10.00 mm, isocratic solvents of various proportions of CH$_3$CN in H$_2$O, 4.0 mL min$^{-1}$, to yield 23 pure compounds: **8** (7.2 mg, 0.14% yield) and **20** (1.0 mg, 0.02% yield) from subfraction 2 (13.1 mg); **7** (2.3 mg, 0.05% yield) and **14** (3.2 mg, 0.06% yield) from subfraction 3 (14.2 mg); **19** (2.8 mg, 0.06% yield) and **23** (13.5 mg, 0.27% yield) from subfraction 5 (23.5 mg); **11** (56.9 mg, 1.14% yield), **15** (2.8 mg, 0.06% yield), **18** (1.0 mg, 0.02% yield), and **21** (3.5 mg, 0.07% yield) from subfraction 6 (85.1 mg); **5** (2.8 mg, 0.07% yield), **9** (2.0 mg, 0.04% yield), and **17** (1.7 mg, 0.03% yield) from subfraction 7 (12.5 mg); **4** (2.3 mg, 0.05% yield), **12** (1.2 mg, 0.02% yield), **24** (1.0 mg, 0.02% yield), and **27** (5.5 mg, 0.11% yield) from subfraction 8 (12.6 mg); **16** (1.9 mg, 0.04% yield) and **25** (9.8 mg, 0.20% yield) from subfraction 9 (18.0 mg); **10** (49.7 mg, 1.00% yield), **26** (3.4 mg, 0.07% yield), **28** (1.3 mg, 0.03% yield), and **29** (3.8 mg, 0.08% yield) from subfraction 11 (69.0 mg).

**Mycalenitrile-4 (4):** amorphous powder; UV (MeOH) $\lambda_{max}$ (log $\varepsilon$) 201 (4.28), 250 (3.78), 301 (4.21) nm; IR (film) $\nu_{max}$ 3260, 2912, 2848, 2246, 1635, 1496, 1352, 1185, 1040, 772, 719 cm$^{-1}$; $^1$H and $^{13}$C NMR, see Tables 1 and 4, respectively; HRESIMS *m/z* 461.3514 [M + Na]$^+$ (calcd for C$_{29}$H$_{46}$N$_2$ONa, 461.3508).

**Mycalenitrile-5 (5):** viscous liquid; UV (MeOH) $\lambda_{max}$ (log $\varepsilon$) 202 (4.13), 250 (3.60), 301 (4.22) nm; IR (film) $\nu_{max}$ 3253, 2923, 2852, 2250, 1641, 1496, 1186, 1041, 772, 720 cm$^{-1}$; $^1$H and $^{13}$C NMR, see Tables 1 and 4, respectively; GC-EIMS (70 eV) *m/z* 438 [M]$^+$ (86.5),

**Table 5.** $^{13}$C NMR Data$^a$ ($\delta$, DEPT) for **6**, **8**, **9**, and **19−21**

| C | 6 | 8 | 9 | 19 | 20 | 21 |
|---|---|---|---|---|---|---|
| 1 | 178.3, CH | 178.3, CH | 178.3, CH | 178.3, CH | 178.3, CH | 178.4, CH |
| 2 | 132.1, C | 132.1, C | 132.1, C | 132.1, C | 132.2, C | 132.2, C |
| 3 | 122.4, CH | 122.8, CH | 122.6, CH | 122.7, CH | 122.8, CH | 122.8, CH |
| 4 | 109.7, CH | 109.6, CH | 109.6, CH | 109.6, CH | 109.6, CH | 109.6, CH |
| 5 | 142.6, C | 143.3, C | 142.9, C | 143.2, C | 142.8, C | 143.2, C |
| 6 | 28.0, CH$_2$ | 28.1, CH$_2$ | 28.1, CH$_2$ | 28.1, CH$_2$ | 28.1, CH$_2$ | 28.1, CH$_2$ |
| 7 | 28.7, CH$_2$ | 29.0, CH$_2$ | 29.0, CH$_2$ | 29.2, CH$_2$ | 29.1, CH$_2$ | 29.1, CH$_2$ |
| 8 | 29.9−29.0$^b$ | 29.9−29.5$^b$ | 30.0−29.4$^b$ | 29.9−29.5$^b$ | 29.8−29.3$^b$ | 29.8−29.4 |
| 9 | 29.9−29.0$^b$ | 29.9−29.5$^b$ | 30.0−29.4$^b$ | 29.9−29.5$^b$ | 29.8−29.3$^b$ | 29.8−29.4 |
| 10 | 29.9−29.0$^b$ | 29.9−29.5$^b$ | 30.0−29.4$^b$ | 29.9−29.5$^b$ | 29.8−29.3$^b$ | 29.8−29.4 |
| 11 | 29.9−29.0$^b$ | 29.9−29.5$^b$ | 30.0−29.4$^b$ | 29.9−29.5$^b$ | 29.8−29.3$^b$ | 29.8−29.4 |
| 12 | 29.9−29.0$^b$ | 29.9−29.5$^b$ | 30.0−29.4$^b$ | 29.9−29.5$^b$ | 27.4, CH$_2$ | 29.8−29.4 |
| 13 | 29.9−29.0$^b$ | 29.9−29.5$^b$ | 30.0−29.4$^b$ | 29.9−29.5$^b$ | 128.0, CH | 29.8−29.4 |
| 14 | 29.9−29.0$^b$ | 29.9−29.5$^b$ | 30.0−29.4$^b$ | 27.4, CH$_2$ | 130.4, CH | 27.4, CH$_2$ |
| 15 | 27.5, CH$_2$ | 29.1, CH$_2$ | 30.0−29.4$^b$ | 128.4, CH$^b$ | 25.8, CH$_2$$^c$ | 127.9, CH |
| 16 | 128.0, CH | 27.4, CH$_2$$^c$ | 30.0−29.4$^b$ | 130.3, CH | 128.5, CH$^d$ | 130.6, CH |
| 17 | 130.5, CH | 130.4, CH$^d$ | 29.2, CH$_2$$^e$ | 25.9, CH$_2$ | 128.4, CH$^d$ | 25.8, CH$_2$$^c$ |
| 18 | 25.9, CH$_2$ | 129.6, CH$^d$ | 27.4, CH$_2$$^c$ | 128.2, CH$^b$ | 25.7, CH$_2$$^c$ | 128.5, CH |
| 19 | 128.9, CH | 27.2, CH$_2$$^c$ | 130.5, CH$^d$ | 130.1, CH | 127.3, CH | 128.5, CH |
| 20 | 129.5, CH | 29.1, CH$_2$ | 129.8, CH$^d$ | 29.4, CH$_2$ | 132.0, CH | 25.7, CH$_2$$^c$ |
| 21 | 27.0, CH$_2$ | 29.9−29.5$^b$ | 27.2, CH$_2$$^c$ | 23.0, CH$_2$ | 20.8, CH$_2$ | 127.3, CH |
| 22 | 28.9, CH$_2$ | 28.9, CH$_2$ | 29.1, CH$_2$$^e$ | 14.0, CH$_3$ | 14.5, CH$_3$ | 132.0, CH |
| 23 | 25.6, CH$_2$ | 25.6, CH$_2$ | 30.0−29.4$^b$ | | | 20.8, CH$_2$ |
| 24 | 17.4, CH$_2$ | 17.3, CH$_2$ | 28.9, CH$_2$ | | | 14.5, CH$_3$ |
| 25 | 120.1, C | 120.0, C | 25.6, CH$_2$ | | | |
| 26 | | | 17.3, CH$_2$ | | | |
| 27 | | | 120.0, C | | | |

$^a$ Bruker AMX 100 MHz spectrometer; $\delta$ values are reported in ppm referenced to CDCl$_3$ ($\delta_C$ 77.23) as internal standard; numerical order groups compounds of similar chain length. $^b$ All carbons were CH$_2$. $^{c−e}$ Values may be interchanged.

409 (36.3), 370 (58.0), 356 (8.3), 342 (9.8), 316 (15.1), 290 (10.3), 276 (3.0), 237 (25.5), 176 (13,9), 148 (24.4), 136 (6.8), 122 (100), 108 (54.1), 96 (15.2), 82 (3.4), 80 (63.5), 41 (10.1); HRESIMS $m/z$ 461.3506 [M + Na]$^+$ (calcd for C$_{29}$H$_{46}$N$_2$ONa, 461.3508).

**Mycalenitrile-6 (6):** colorless oil; UV (MeOH) $\lambda_{max}$ (log $\varepsilon$) 203 (4.10), 235 (3.90), 301 (4.20) nm; IR (film) $\nu_{max}$ 3254, 2917, 2849, 2252, 1641, 1465, 1186, 1041, 719 cm$^{-1}$; $^1$H and $^{13}$C NMR, see Tables 2 and 5, respectively; GC-EIMS (70 eV) $m/z$ 382 [M]$^+$ (41.3), 353 (9.1), 300 (10.0), 260 (18.4), 234 (6.5), 202 (10.8), 162 (14.8), 148 (8.8), 136 (8.7), 122 (65.5), 108 (53.7), 96 (100), 82 (11.1), 80 (66.0), 41 (73.4); HRESIMS $m/z$ 405.2865 [M + Na]$^+$ (calcd for C$_{25}$H$_{38}$N$_2$ONa, 405.2882).

**Mycalenitrile-7 (7):** colorless oil; UV (MeOH) $\lambda_{max}$ (log $\varepsilon$) 201 (4.02), 242 (3.87), 301 (4.23) nm; IR (film) $\nu_{max}$ 3256, 2924, 2853, 2248, 1640, 1496, 1186, 1041, 772, 721 cm$^{-1}$; $^1$H and $^{13}$C NMR, see Tables 1 and 4, respectively; GC-EIMS (70 eV) $m/z$ 410 [M]$^+$ (64.6), 381 (25.7), 355 (23.9), 328 (19.9), 262 (4.8), 194 (19.1), 148 (32.5), 136 (2.7), 122 (100), 108 (85.0), 96 (36.1), 82 (24.1), 80 (91.2), 41 (76.9); HRESIMS $m/z$ 433.3207 [M + Na]$^+$ (calcd for C$_{27}$H$_{42}$N$_2$ONa, 433.3195).

**Mycalenitrile-8 (8):** yellow solid, mp 42−44 °C; UV (MeOH) $\lambda_{max}$ (log $\varepsilon$) 201 (3.78), 250 (3.51), 301 (4.18) nm; IR (film) $\nu_{max}$ 3180, 2920, 2850, 2246, 1642, 1495, 1044, 778 cm$^{-1}$; $^1$H and $^{13}$C NMR, see Tables 2 and 5, respectively; GC-EIMS (70 eV) $m/z$ 384 [M]$^+$ (48.5), 355 (49.0), 302 (28.3), 288 (100), 234 (18.5), 150 (39.5), 122 (82.0), 108 (65.8), 80 (75.0), 41 (23.2); HRESIMS $m/z$ 407.3041 [M + Na]$^+$ (calcd for C$_{25}$H$_{40}$N$_2$ONa, 407.3038).

**Mycalenitrile-9 (9):** colorless oil; UV (MeOH) $\lambda_{max}$ (log $\varepsilon$) 201 (3.78), 250 (3.53), 301 (4.17) nm; IR (film) $\nu_{max}$ 3247, 2921, 2851, 2245, 1637, 1499, 1043, 773 cm$^{-1}$; $^1$H and $^{13}$C NMR, see Tables 2 and 5, respectively; GC-EIMS (70 eV) $m/z$ 412 [M]$^+$ (85.7), 383 (27.9), 344 (2.8), 330 (12.5), 316 (9.6), 302 (2.3), 262 (18.8), 248 (5.8), 150 (18.6), 122 (100), 109 (43.0), 108 (66.6), 96 (17.2), 94 (15.9), 80 (18.6), 55 (18.5); HRESIMS $m/z$ 435.3362 [M + Na]$^+$ (calcd for C$_{27}$H$_{44}$N$_2$ONa, 435.3371).

**Mycalenitrile-10 (10):** white solid, mp 42−45 °C; UV (MeOH) $\lambda_{max}$ (log $\varepsilon$) 202 (3.76), 250 (3.55), 301 (4.20) nm; IR (film) $\nu_{max}$ 3217, 2920, 2851, 2246, 1642, 1495, 1043, 778 cm$^{-1}$; $^1$H and $^{13}$C NMR, see Tables 1 and 4, respectively; GC-EIMS (70 eV) $m/z$ 440 [M]$^+$ (47.6), 411 (24.8), 355 (23.9), 344 (28.8), 290 (55.3), 207 (100), 192 (18.6), 150 (24.9), 122 (34.9), 109 (15.2), 108 (29.8), 96 (18.6), 94 (10.2), 80 (50.8), 55 (20.7); HRESIMS $m/z$ 463.3672 [M + Na]$^+$ (calcd for C$_{29}$H$_{48}$N$_2$ONa, 463.3664).

**Mycalenitrile-11 (11):** colorless oil; UV (MeOH) $\lambda_{max}$ (log $\varepsilon$) 202 (3.76), 250 (3.52), 302 (4.23) nm; IR (film) $\nu_{max}$ 3244, 2920, 2851, 2244, 1637, 1500, 1043, 774 cm$^{-1}$; $^1$H and $^{13}$C NMR, see Tables 1 and 4, respectively; GC-EIMS (70 eV) $m/z$ 412 [M]$^+$ (74.4), 383 (28.8), 344 (4.9), 330 (12.8), 316 (13.0), 302 (3.3), 288 (3.0), 274 (2.9), 260 (3.7), 246 (6.5), 232 (5.5), 218 (6.5), 204 (6.5), 190 (4.9), 178 (11.6), 164 (11.3), 150 (19.5), 122 (100), 108 (58.7), 80 (48.5), 55 (16.0), 41 (11.0); HRESIMS $m/z$ 435.3348 [M + Na]$^+$ (calcd for C$_{27}$H$_{44}$N$_2$ONa, 435.3351).

**Mycalenitrile-12 (12):** colorless oil; UV (MeOH) $\lambda_{max}$ (log $\varepsilon$) 201 (3.74), 250 (3.53), 301 (4.16) nm; IR (film) $\nu_{max}$ 3251, 2918, 2850, 2245, 1636, 1494, 1041, 771 cm$^{-1}$; $^1$H and $^{13}$C NMR, see Tables 1 and 4, respectively; GC-EIMS (70 eV) $m/z$ 426 [M]$^+$ (100), 397 (34.9), 358 (3.4), 344 (16.3), 330 (16.5), 316 (3.3), 302 (3.2), 288 (2.9), 274 (3.4), 260 (4.0), 246 (5.7), 232 (6.6), 218 (6.6), 204 (7.5), 190 (5.3), 178 (13.0), 164 (12.2), 150 (14.9), 122 (93.1), 108 (51.3), 80 (39.3), 55 (13.4), 41 (7.6); HRESIMS $m/z$ 449.3519 [M + Na]$^+$ (calcd for C$_{28}$H$_{46}$N$_2$ONa, 449.3508).

**Mycalenitrile-13 (13):** white solid, mp 73−75 °C; UV (MeOH) $\lambda_{max}$ (log $\varepsilon$) 201 (3.78), 247 (3.43), 301 (4.20) nm; IR (film) $\nu_{max}$ 3172, 2920, 2849, 2247, 1642, 1495, 1043, 780 cm$^{-1}$; $^1$H and $^{13}$C NMR, see Tables 3 and 6, respectively; HRESIMS $m/z$ 331.2750 [M]$^+$ (calcd for C$_{21}$H$_{34}$N$_2$O, 331.2749).

**Mycalenitrile-14 (14):** white solid, mp 74−77 °C; UV (MeOH) $\lambda_{max}$ (log $\varepsilon$) 201 (3.77), 249 (3.47), 301 (4.03) nm; IR (film) $\nu_{max}$ 3178, 2921, 2848, 2245, 1645, 1494, 1043, 781, 725 cm$^{-1}$; $^1$H and $^{13}$C NMR, see Tables 3 and 6, respectively; HRESIMS $m/z$ 395.3012 [M + Na]$^+$ (calcd for C$_{24}$H$_{40}$N$_2$ONa, 395.3038).

**Mycalazal-14 (15):** amorphous powder; UV (MeOH) $\lambda_{max}$ (log $\varepsilon$) 201 (3.72), 250 (3.46), 301 (4.18) nm; IR (film) $\nu_{max}$ 3174, 2921, 2849, 1645, 1494, 1043, 778, 724 cm$^{-1}$; $^1$H and $^{13}$C NMR, see Tables 3 and 6, respectively; HRESIMS $m/z$ 314.2450 [M + Na]$^+$ (calcd for C$_{19}$H$_{33}$NONa, 314.2460).

**Mycalazal-15 (16):** colorless oil; UV (MeOH) $\lambda_{max}$ (log $\varepsilon$) 201 (3.86), 250 (3.75), 301 (4.08) nm; IR (film) $\nu_{max}$ 3257, 2928, 2856, 1643, 1498, 1187, 1042, 772 cm$^{-1}$; $^1$H and $^{13}$C NMR, see Tables 3 and 6, respectively; GC-EIMS (70 eV) $m/z$ 331 [M]$^+$ (100), 302 (12.2), 260 (7.2), 206 (3.6), 192 (4.2), 178 (8.8), 164 (9.4), 150 (23.1), 122 (59.8), 108 (78.2), 80 (70.6), 55 (21.5); HRESIMS $m/z$ 354.2748 [M + Na]$^+$ (calcd for C$_{22}$H$_{37}$NONa, 354.2773).

**Mycalazal-16 (17):** colorless oil; UV (MeOH) $\lambda_{max}$ (log $\varepsilon$) 201 (3.92), 249 (3.76), 301 (4.22) nm; IR (film) $\nu_{max}$ 3253, 2920, 2851, 1637, 1494, 1185, 1041, 771 cm$^{-1}$; $^1$H and $^{13}$C NMR, see Tables 3

**Table 6.** $^{13}$C NMR Data$^a$ ($\delta$, DEPT) for **13−18**

| C | 13 | 14 | 15 | 16 | 17 | 18 |
|---|---|---|---|---|---|---|
| 1 | 178.3, CH | 178.3, CH | 178.3, CH | 178.3, CH | 178.4, CH | 178.4, CH |
| 2 | 132.1, C | 132.0, C | 132.0, C | 132.1, C | 132.2, C | 132.1, C |
| 3 | 122.7, CH | 122.8, CH | 122.8, CH | 122.6, CH | 122.8, CH | 122.8, CH |
| 4 | 109.7, CH | 109.6, CH | 109.6, CH | 109.6, CH | 109.7, CH | 109.7, CH |
| 5 | 143.3, C | 143.4, C | 143.3, C | 143.0, C | 142.8, C | 142.4, C |
| 6 | 28.1, CH$_2$ | 28.1, CH$_2$ | 28.1, CH$_2$ | 28.1, CH$_2$ | 28.1, CH$_2$ | 28.0, CH$_2$ |
| 7 | 29.2, CH$_2$ | 29.2, CH$_2$ | 29.1, CH$_2$ | 29.1, CH$_2$ | 26.9, CH$_2$ | 28.7, CH$_2$ |
| 8 | 29.8−29.4$^b$ | 29.9−29.4$^b$ | 29.9−29.4$^b$ | 30.0−29.2$^b$ | 127.7, CH | 29.8−29.2$^b$ |
| 9 | 29.8−29.4$^b$ | 29.9−29.4$^b$ | 29.9−29.4$^b$ | 30.0−29.2$^b$ | 132.4, CH | 29.8−29.2$^b$ |
| 10 | 29.8−29.4$^b$ | 29.9−29.4$^b$ | 29.9−29.4$^b$ | 30.0−29.2$^b$ | 27.5, CH$_2$ | 29.8−29.2$^b$ |
| 11 | 29.8−29.4$^b$ | 29.9−29.4$^b$ | 29.9−29.4$^b$ | 30.0−29.2$^b$ | 30.2−29.4$^b$ | 27.5, CH$_2$ |
| 12 | 29.8−29.4$^b$ | 29.9−29.4$^b$ | 29.9−29.4$^b$ | 30.0−29.2$^b$ | 30.2−29.4$^b$ | 130.8, CH$^c$ |
| 13 | 29.8−29.4$^b$ | 29.9−29.4$^b$ | 29.9−29.4$^b$ | 30.0−29.2$^b$ | 30.2−29.4$^b$ | 129.2, CH$^c$ |
| 14 | 29.8−29.4$^b$ | 29.9−29.4$^b$ | 29.9−29.4$^b$ | 27.4, CH$_2$ | 30.2−29.4$^b$ | 27.5, CH$_2$ |
| 15 | 29.8−29.4$^b$ | 29.9−29.4$^b$ | 29.9−29.4$^b$ | 130.2, CH$^b$ | 30.2−29.4$^b$ | 29.8−29.2 |
| 16 | 29.8−29.4$^b$ | 29.9−29.4$^b$ | 29.9−29.4$^b$ | 130.1, CH$^b$ | 30.2−29.4$^b$ | 29.8−29.2 |
| 17 | 29.8−29.4$^b$ | 29.9−29.4$^b$ | 32.1, CH$_2$ | 27.4, CH$_2$ | 30.2−29.4$^b$ | 29.8−29.2 |
| 18 | 28.9, CH$_2$ | 29.9−29.4$^b$ | 22.9, CH$_2$ | 30.0−29.2$^b$ | 39.2, CH$_2$ | 39.2, CH$_2$ |
| 19 | 25.6, CH$_2$ | 29.9−29.4$^b$ | 14.3, CH$_3$ | 30.0−29.2$^b$ | 27.7, CH$_2$ | 27.7, CH$_2$ |
| 20 | 17.3, CH$_2$ | 29.9−29.4$^b$ | | 32.0, CH$_2$ | 22.9, CH$_3$ | 22.9, CH$_3$ |
| 21 | 120.0, C | 28.9, CH$_2$ | | 22.9, CH$_2$ | 22.9, CH$_3$ | 22.9, CH$_3$ |
| 22 | | 25.6, CH$_2$ | | 14.3, CH$_3$ | | |
| 23 | | 17.3, CH$_2$ | | | | |
| 24 | | 120.1, C | | | | |

$^a$ Bruker AMX 100 MHz spectrometer; $\delta$ values are reported in ppm referenced to CDCl$_3$ ($\delta_C$ 77.23) as internal standard; numerical order groups compounds of similar chain length; $^b$ Carbons were CH$_2$; $^c$ Values may be interchanged.

and 6, respectively; HRESIMS $m/z$ 340.2641 [M + Na]$^+$ (calcd for C$_{21}$H$_{35}$NONa 340.2616).

**Mycalazal-17 (18):** colorless oil; UV (MeOH) $\lambda_{max}$ (log $\varepsilon$) 202 (3.87), 249 (3.72), 301 (4.18) nm; IR (film) $\nu_{max}$ 3256, 2924, 2853, 1643, 1497, 1187, 1042, 772 cm$^{-1}$; $^1$H and $^{13}$C NMR, see Tables 3 and 6, respectively; GC-EIMS (70 eV) $m/z$ 317 [M]$^+$ (40.0), 288 (18.5), 274 (5.4), 250 (2.7), 246 (2.3), 232 (3.3), 221 (51.0), 218 (7.5), 204 (12.2), 190 (11.0), 178 (2.3), 164 (9.0), 150 (22.8), 122 (100), 108 (19.8), 96 (25.1), 80 (69.2), 55 (28.2); HRESIMS $m/z$ 340.2625 [M + Na]$^+$ (calcd for C$_{21}$H$_{35}$NONa, 340.2616).

**Mycalazal-18 (19):** colorless oil; UV (MeOH) $\lambda_{max}$ (log $\varepsilon$) 201 (4.17), 241 (3.60), 301 (4.19) nm; IR (film) $\nu_{max}$ 3255, 2923, 2853, 1641, 1496, 1186, 1042, 772, 719 cm$^{-1}$; $^1$H and $^{13}$C NMR, see Tables 2 and 5, respectively; HRESIMS $m/z$ 352.2621 [M + Na]$^+$ (calcd for C$_{22}$H$_{35}$NONa, 352.2611).

**Mycalazal-19 (20):** colorless oil; UV (MeOH) $\lambda_{max}$ (log $\varepsilon$) 201 (4.24), 237 (3.80), 301 (4.20) nm; IR (film) $\nu_{max}$ 3248, 2925, 2854, 1637, 1497, 1186, 1041, 772 cm$^{-1}$; $^1$H and $^{13}$C NMR, see Tables 2 and 5, respectively; HRESIMS $m/z$ 350.2456 [M + Na]$^+$ (calcd for C$_{22}$H$_{33}$NONa, 350.2454).

**Mycalazal-20 (21):** colorless oil; UV (MeOH) $\lambda_{max}$ (log $\varepsilon$) 201 (4.29), 241 (3.82), 301 (4.17) nm; IR (film) $\nu_{max}$ 3254, 2924, 2853, 1641, 1497, 1187, 1042, 772, 720 cm$^{-1}$; $^1$H and $^{13}$C NMR, see Tables 2 and 5, respectively; HRESIMS $m/z$ 378.2780 [M + Na]$^+$ (calcd for C$_{24}$H$_{37}$NONa, 378.2767).

**Cell-Based Reporter Assay.** The maintenance of human breast tumor T47D (ATCC) cells and the T47D cell-based reporter assay for HIF-1 activity were described previously.[23−25] The extract and the fractions were dissolved in DMSO, and the final solvent concentration is less than 0.5%. The pure compounds were dissolved in 2-propanol at 4 mM and the stock solutions stored at −20 °C. Final solvent concentration is less than 0.75%. The following formula was used to calculate the % inhibition data:

$$\% \text{ inhibition} = (1 - \text{light output}_{\text{treated}} / \text{light output}_{\text{induced}}) \times 100$$

**ELISA Assay for VEGF Protein.** The detailed procedure was described previously.[24,25] The data were presented as the level of secreted VEGF proteins in the conditioned media normalized to the quantity of total proteins in the cell lysate determined by a micro BCA assay (Pierce).

**Mitochondria Respiration Assay.** As previously described,[24,25] a method used to monitor the respiration of isolated mitochondria was modified to measure the level of oxygen consumption in intact or digitonin-permeabilized T47D cells and to investigate the specific target within the mitochondrial electron transport chain affected by active compounds. The known ETC inhibitors—rotenone for complex I and antimycin A for complex III—were prepared as stock solutions in ethanol and added to final concentrations of 1 $\mu$M where indicated.

**Cell Proliferation/Viability Assay.** The maintenance of T47D and MDA-MB-231 cells (ATCC), cell plating, compound addition, exposure to specified oxygen conditions, and determination of cell proliferation/viability with the sulforhodamine B method were the same as those described.[25] A BioTek Synergy plate reader was used to measure light absorbance at 490 nm with background absorbance at 690 nm. To calculate the percentage inhibition data, a formula similar to the one stated in the reporter assay was used. All compound-treated samples were compared to the media control under each specified oxygen condition.

**Statistical Analysis.** Data were compared using one-way ANOVA and Bonfferoni post hoc analyses (GraphPad Prism 4). Differences were considered significant when $p < 0.05$.

**Supporting Information Available:** Spectroscopic data ($^1$H and $^{13}$C NMR) for **4−21**. The material is available free of charge via the Internet at http://pubs.acs.org.

**References and Notes**

(1) Bache, M.; Kappler, M.; Said, H. M.; Staab, A.; Vordermark, D. *Curr. Med. Chem.* **2008**, *15*, 322–338.
(2) Tatum, J. L.; Kelloff, G. J.; Gillies, R. J.; Arbeit, J. M.; Brown, J. M.; Chao, K. S.; Chapman, J. D.; Eckelman, W. C.; Fyles, A. W.; Giaccia, A. J.; Hill, R. P.; Koch, C. J.; Krishna, M. C.; Krohn, K. A.; Lewis, J. S.; Mason, R. P.; Melillo, G.; Padhani, A. R.; Powis, G.; Rajendran, J. G.; Reba, R.; Robinson, S. P.; Semenza, G. L.; Swartz, H. M.; Vaupel, P.; Yang, D.; Croft, B.; Hoffman, J.; Liu, G.; Stone, H.; Sullivan, D. *Int. J. Radiat. Biol.* **2006**, *82*, 699–757.

(3) Semenza, G. L.; Wang, G. L. *Mol. Cell. Biol.* **1992**, *12*, 5447–5454.

(4) Wang, G. L.; Semenza, G. L. *J. Biol. Chem.* **1995**, *270*, 1230–1237.

(5) Semenza, G. L. *IUBMB Life* **2008**, *60*, 591–597.

(6) Rankin, E. B.; Giaccia, A. J. *Cell Death Differ.* **2008**, *15*, 678–685.

(7) Semenza, G. L. *Drug Discovery Today* **2007**, *12*, 853–859.

(8) Wang, G. L.; Jiang, B. H.; Rue, E. A.; Semenza, G. L. *Proc. Natl. Acad. Sci. U.S.A.* **1995**, *92*, 5510–5514.

(9) Maxwell, P. H.; Wiesener, M. S.; Chang, G. W.; Clifford, S. C.; Vaux, E. C.; Cockman, M. E.; Wykoff, C. C.; Pugh, C. W.; Maher, E. R.; Ratcliffe, P. J. *Nature* **1999**, *399*, 271–275.

(10) Ivan, M.; Kondo, K.; Yang, H.; Kim, W.; Valiando, J.; Ohh, M.; Salic, A.; Asara, J. M.; Lane, W. S.; Kaelin, W. G. *Science* **2001**, *292*, 464–468.

(11) Jaakkola, P.; Mole, D. R.; Tian, Y. M.; Wilson, M. I.; Gielbert, J.; Gaskell, S. J.; Kriegsheim, A.; Hebestreit, H. F.; Mukherji, M.; Schofield, C. J.; Maxwell, P. H.; Pugh, C. W.; Ratcliffe, P. J. *Science* **2001**, *292*, 468–472.

(12) Epstein, A. C.; Gleadle, J. M.; McNeill, L. A.; Hewitson, K. S.; O'Rourke, J.; Mole, D. R.; Mukherji, M.; Metzen, E.; Wilson, M. I.; Dhanda, A.; Tian, Y. M.; Masson, N.; Hamilton, D. L.; Jaakkola, P.; Barstead, R.; Hodgkin, J.; Maxwell, P. H.; Pugh, C. W.; Schofield, C. J.; Ratcliffe, P. J. *Cell* **2001**, *107*, 43–54.

(13) Bruick, R. K.; McKnight, S. L. *Science* **2001**, *294*, 1337–1340.

(14) Lando, D.; Peet, D. J.; Whelan, D. A.; Gorman, J. J.; Whitelaw, M. L. *Science* **2002**, *295*, 858–861.

(15) Ryan, H. E.; Poloni, M.; McNulty, W.; Elson, D.; Gassmann, M.; Arbeit, J. M.; Johnson, R. S. *Cancer Res.* **2000**, *60*, 4010–4015.

(16) Rapisarda, A.; Zalek, J.; Hollingshead, M.; Braunschweig, T.; Uranchimeg, B.; Bonomi, C. A.; Borgel, S. D.; Carter, J. P.; Hewitt, S. M.; Shoemaker, R. H.; Melillo, G. *Cancer Res.* **2004**, *64*, 6845–6848.

(17) Greenberger, L. M.; Horak, I. D.; Filpula, D.; Sapra, P.; Westergaard, M.; Frydenlund, H. F.; Albaek, C.; Schroder, H.; Orum, H. *Mol. Cancer Ther.* **2008**, *7*, 3598–3608.

(18) Unruh, A.; Ressel, A.; Mohamed, H. G.; Johnson, R. S.; Nadrowitz, R.; Richter, E.; Katschinski, D. M.; Wenger, R. H. *Oncogene* **2003**, *22*, 3213–3220.

(19) Moeller, B. J.; Dreher, M. R.; Rabbani, Z. N.; Schroeder, T.; Cao, Y.; Li, C. Y.; Dewhirst, M. W. *Cancer Cell* **2005**, *8*, 99–110.

(20) Li, L.; Lin, X.; Shoemaker, A. R.; Albert, D. H.; Fesik, S. W.; Shen, Y. *Clin. Cancer Res.* **2006**, *12*, 4747–4754.

(21) Cairns, R. A.; Papandreou, I.; Sutphin, P. D.; Denko, N. C. *Proc. Natl. Acad. Sci. U.S.A.* **2007**, *104*, 9445–9450.

(22) U.S. NIH database ClinicalTrials.gov, http://www.clinicaltrials.gov/ct2/search, accessed July 22, 2009.

(23) Hodges, T. W.; Hossain, C. F.; Kim, Y. P.; Zhou, Y. D.; Nagle, D. G. *J. Nat. Prod.* **2004**, *67*, 767–771.

(24) Liu, Y.; Liu, R.; Mao, S. C.; Morgan, J. B.; Jekabsons, M. B.; Zhou, Y. D.; Nagle, D. G. *J. Nat. Prod.* **2008**, *71*, 1854–1860.

(25) Liu, Y.; Veena, C. K.; Morgan, J. B.; Mohammed, K. A.; Jekabsons, M. B.; Nagle, D. G.; Zhou, Y. D. *J. Biol. Chem.* **2009**, *284*, 5859–5868.

(26) West, L. M.; Northcote, P. T.; Battershill, C. N. *J. Org. Chem.* **2000**, *65*, 445–449.

(27) Hood, K. A.; West, L. M.; Rouwe, B.; Northcote, P. T.; Berridge, M. V.; Wakefield, S. J.; Miller, J. H. *Cancer Res.* **2002**, *62*, 3356–3360.

(28) Huzil, J. T.; Chik, J. K.; Slysz, G. W.; Freedman, H.; Tuszynski, J.; Taylor, R. E.; Sackett, D. L.; Schriemer, D. C. *J. Mol. Biol.* **2008**, *378*, 1016–1030.

(29) Northcote, P. T. B., J. W.; Munro, H. G. *Tetrahedron Lett.* **1991**, *32*, 6411–6414.

(30) Low, W. K.; Dang, Y.; Schneider-Poetsch, T.; Shi, Z.; Choi, N. S.; Merrick, W. C.; Romo, D.; Liu, J. O. *Mol. Cell* **2005**, *20*, 709–722.

(31) Bordeleau, M. E.; Matthews, J.; Wojnar, J. M.; Lindqvist, L.; Novac, O.; Jankowsky, E.; Sonenberg, N.; Northcote, P.; Teesdale-Spittle, P.; Pelletier, J. *Proc. Natl. Acad. Sci. U.S.A.* **2005**, *102*, 10460–10465.

(32) Maulucci, N.; Chini, M. G.; Micco, S. D.; Izzo, I.; Cafaro, E.; Russo, A.; Gallinari, P.; Paolini, C.; Nardi, M. C.; Casapullo, A.; Riccio, R.; Bifulco, G.; Riccardis, F. D. *J. Am. Chem. Soc.* **2007**, *129*, 3007–3012.

(33) Nakao, Y.; Yoshida, S.; Matsunaga, S.; Shindoh, N.; Terada, Y.; Nagai, K.; Yamashita, J. K.; Ganesan, A.; van Soest, R. W.; Fusetani, N. *Angew. Chem., Int. Ed.* **2006**, *45*, 7553–7557.

(34) Ortega, M. J.; Zubía, E.; Sánchez, M. C.; Salvá, J.; Carballo, J. L. *Tetrahedron* **2004**, *60*, 2517–2524.

(35) Compagnone, R. S.; Oliveri, M. C.; Piña, I.; Marques, S.; Rangel, H. R.; Dagger, F.; Suárez, A. I.; Gómez, M. *Nat. Prod. Lett.* **1999**, *13*, 203–211.

(36) Stierle, D. B.; Faulkner, D. J. *J. Org. Chem.* **1980**, *45*, 4980–4982.

(37) Breitmaier, E.; Voelter, W. In *Carbon-13 NMR Spectroscopy*, 3rd ed.; VCH: New York, 1989; pp 192−194.

(38) Venkatesham, U.; Rao, M. R.; Venkateswarlu, Y. *J. Nat. Prod.* **2000**, *63*, 1318–1320.

(39) Ferrara, N.; Mass, R. D.; Campa, C.; Kim, R. *Annu. Rev. Med.* **2007**, *58*, 491–504.

(40) Nagle, D. G.; Zhou, Y. D. *Curr. Drug Targets* **2006**, *7*, 355–369.

(41) Lin, X.; David, C. A.; Donnelly, J. B.; Michaelides, M.; Chandel, N. S.; Huang, X.; Warrior, U.; Weinberg, F.; Tormos, K. V.; Fesik, S. W.; Shen, Y. *Proc. Natl. Acad. Sci. U.S.A.* **2008**, *105*, 174–179.

(42) Guzy, R. D.; Hoyos, B.; Robin, E.; Chen, H.; Liu, L.; Mansfield, K. D.; Simon, M. C.; Hammerling, U.; Schumacker, P. T. *Cell Metab.* **2005**, *1*, 401–408.

(43) Simon, M. C. *Adv. Exp. Med. Biol.* **2006**, *588*, 165–170.

(44) Pan, Y.; Mansfield, K. D.; Bertozzi, C. C.; Rudenko, V.; Chan, D. A.; Giaccia, A. J.; Simon, M. C. *Mol. Cell. Biol.* **2007**, *27*, 912–925. Bell, E. L.; Klimova, T. A.; Eisenbart, J.; Moraes, C. T.; Murphy, M. P.; Budinger, G. R. S.; Chandel, N. S. *J. Cell Biol.* **2007**, *177*, 1029–1036.